SIAM J. NUMER. ANAL.
Vol. 51, No. 6, pp. 3062–3083

CONDITION NUMBER ESTIMATES FOR THE NONOVERLAPPING OPTIMIZED SCHWARZ METHOD AND THE 2-LAGRANGE MULTIPLIER METHOD FOR GENERAL DOMAINS AND CROSS POINTS*

SÉBASTIEN LOISEL†

Abstract. The optimized Schwarz method and the closely related 2-Lagrange multiplier method are domain decomposition methods which can be used to parallelize the solution of partial differential equations. Although these methods are known to work well in special cases (e.g., when the domain is a square and the two subdomains are rectangles), the problem has never been systematically stated nor analyzed for general domains with general subdomains. The problem of cross points (when three or more subdomains meet at a single vertex) has been particularly vexing. We introduce a 2-Lagrange multiplier method for domain decompositions with cross points. We estimate the condition number of the iteration and provide an optimized Robin parameter for general domains. We hope that this new systematic theory will allow broader utilization of optimized Schwarz and 2-Lagrange multiplier preconditioners.

Key words. domain decomposition, Schwarz method, partial differential equation, parallel preconditioner, Krylov space, 2-Lagrange multiplier

AMS subject classifications. 35J15, 65F08, 65N55

DOI. 10.1137/100803316

1. Introduction.

In mathematics, physics, and engineering, it is useful to solve elliptic PDEs, such as the Laplace problem

$$\Delta u = f \text{ in } \Omega \text{ and } u = 0 \text{ on } \partial\Omega. \tag{1.1}$$

Such problems are often solved numerically. The discretized problem has the form

$$A\mathbf{u} = \mathbf{f}, \tag{1.2}$$

where A is a large invertible $n \times n$ matrix, $\mathbf{f}$ is a given n-dimensional vector, and $\mathbf{u}$ is the desired solution.

One way to obtain this discretization is to use the finite element method; to fix ideas, we use piecewise linear elements. We then have a set $\phi_1(x), \ldots, \phi_n(x)$ of piecewise linear basis functions, and the solution $u(x)$ is approximated by $u_h(x) = \sum_{k=1}^{n} u_k \phi(x)$, where the vector $\mathbf{u} = \begin{bmatrix} u_1 & \ldots & u_n \end{bmatrix}^T$ is the solution of (1.2). The "stiffness matrix" A has entries $A_{ij} = \int_\Omega \nabla\phi_i \cdot \nabla\phi_j$ while the "forcing" has entries $f_i = \int_\Omega f(x)\phi_i(x)$.

When A is large, it may be desirable to solve it iteratively, by breaking it up into smaller pieces using a domain decomposition method. Such methods are readily made parallel, since each subdomain can be assigned to a separate processor. At the geometric level, a nonoverlapping domain decomposition is a partition of the domain Ω into nonoverlapping parts $\Omega_1, \ldots, \Omega_p$. From this partition, we can further define

*Received by the editors July 23, 2010; accepted for publication (in revised form) July 9, 2013; published electronically November 19, 2013.
http://www.siam.org/journals/sinum/51-6/80331.html

†Department of Mathematics, Heriot-Watt University, Edinburgh, Scotland, EH14 4AS, UK (S.Loisel@hw.ac.uk).

the "artificial interface"

$$\Gamma = \Omega \cap \left(\bigcup_{i=1}^{p} \partial\Omega_i \right).$$

The set $\partial\Omega$ is called the natural boundary, since it is an intrinsic part of the original problem definition. In the present paper, there is a Dirichlet condition on the natural boundary. The interface Γ is artificial in that it bears no relationship to the "physical" problem (1.1). Indeed, it is introduced purely for the purpose of calculation.

The partition $\Omega_1, \ldots, \Omega_p$ can be used to assign the n degrees of freedom of $\mathbf{u}$ to the various subdomains. Although the geometric domain decomposition is nonoverlapping, from the algebraic point of view there is a kind of overlap since degrees of freedom along interfaces may have to be shared between two or more adjacent subdomains. The current article is concerned mainly with such methods, which are nonoverlapping in the geometric (or PDE) interpretation, while at the algebraic level, the degrees of freedom along Γ are shared between the adjacent subdomains.

The main idea of the 2-Lagrange multiplier (2LM) method is to replace the large coupled system (1.2) with many local problems with Robin boundary conditions on the artificial interface. This idea is very similar to the finite element tearing and interconnecting (FETI) method, where Neumann boundary conditions are called "Lagrange multipliers" since they can be regarded as arising from the relaxation of continuity constraints. In the 2LM method, at each vertex of the artificial interface Γ, there are multiple Robin values (one per adjacent subdomain). At a typical "regular" interface vertex, there are two adjacent subdomains, which motivates the terminology of "2-Lagrange multiplier."

A precursor to the 2LM method was introduced in [11] for solving the Helmholtz problems using two Lagrange multipliers with imaginary Robin parameters. In [36], the method was adapted to elliptic problems with positive Robin parameters. The existing literature does not treat the case of cross points, and there is no analysis of condition numbers or convergence properties.

The 2LM method is known to be closely related to the nonoverlapping optimized Schwarz method (OSM). We now briefly outline the history of the OSM; refer to [13] and [14] for details. The OSM was introduced in [12], but we also mention the earlier work [3], [32], [33]. Attempts have been made to find optimized transmission conditions for various differential equations or suitable domains; see, e.g., [18], [21], [22], [23], [24].

For some simple problems and domains, optimized transmission conditions can be found by Fourier analysis. In addition to the Laplace and Helmholtz problems, this Fourier method can be used for various other canonical problems; see [2], [9], [16], [17], [29], [30] for convection-diffusion problems, [15], [19] for the wave equation, [1], [5] for Maxwell's equations, [6] for fluid dynamics, and [31], [34] for the shallow water equation.

Proofs of convergence for more general situations have been recently obtained [25], [28]; but the techniques used are not amenable to finding the optimal parameters. A proof of convergence for the nonoverlapping algorithm without cross points was provided in [26], using energy estimates. (This proof does not provide condition number estimates or optimized parameter values.) We mention in passing that one way of obtaining convergence of the nonoverlapping algorithm is to define a relaxation of the method [4]. There is an ongoing effort to estimate the spectral radius of the optimized Schwarz iteration with cross points; see [20].

All of these methods have been described for domain decompositions without cross points, but the presence of cross points poses a difficulty. OSMs have seen limited deployment in applications. We surmise that this is because of the poorly understood performance of the OSM when there are cross points. It is difficult for practitioners to use the method when it is not even clearly defined. Our major innovation in the present article is to introduce and analyze a systematic method to deal with cross points. Our new methods generalize the nonoverlapping OSM or 2LM method to general domains and subdomains with cross points.

We have three main results. Our first main result is to give a nonoverlapping OSM, or a 2LM system, defined even when there are cross-points. We show that we can recover the solution to the system $A\mathbf{u} = \mathbf{f}$ from the unique solution to this nonoverlapping OSM. This main result is important because the 2LM method, or the nonoverlapping OSM, has never been formulated systematically in the presence of cross points with general subdomains.

Our second main result gives the optimized Robin parameter and a condition number estimate for the nonoverlapping OSM in terms of the spectral properties of local Schur complements. We apply this estimate to a PDE to obtain our third main result. The idea that the condition number could be estimated from the spectral properties of the local Schur complements occurred to us when we were reading [10]. Our original contributions consist of our three main results, including the technically challenging proofs of Lemma 3.2 and 3.6.

Our paper is organized as follows. In section 2, we introduce the 2LM method and show that (1.2) and the 2LM method are equivalent, even if A is nonsymmetric. In section 3, we provide condition number estimates for the 2LM method in terms of algebraic properties of A. In section 4, we give condition number estimates for the case when A is the discretization of an elliptic PDE. In section 5, we verify our estimates with numerical experiments. We end with some conclusions in section 6, which is followed by an appendix.

2. Solving $A\mathbf{u} = \mathbf{f}$ using Robin subproblems. We assume that the domain Ω is in $\mathbb{R}^2$ or $\mathbb{R}^3$ and is discretized using some grid of points $\{\mathbf{x}_1, \ldots, \mathbf{x}_n\}$, as in Figure 2.1. The domain is further partitioned into nonoverlapping subdomains $\Omega_1, \ldots, \Omega_p$ with artificial interface Γ.

To fix ideas, in the remainder of the present paper, we will assume that the vertices are arranged as follows:

$$\overbrace{\mathbf{x}_1, \ldots, \mathbf{x}_{n_{I1}}}^{\in\Omega_1}, \overbrace{\mathbf{x}_{n_{I1}+1}, \ldots, \mathbf{x}_{n_{I1}+n_{I2}}}^{\in\Omega_2}, \ \ldots\ , \overbrace{\mathbf{x}_{n_I-n_{Ip}+1}, \ldots, \mathbf{x}_{n_I}}^{\in\Omega_p}, \overbrace{\mathbf{x}_{n_I+1}, \ldots, \mathbf{x}_n}^{\in\Gamma};$$

see Figure 2.1.

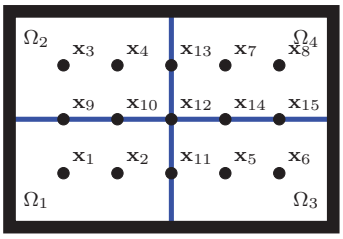

FIG. 2.1. *A discretized rectangular domain with* 15 *grid points. The artificial interface is* $\Gamma = \{\mathbf{x}_9, \ldots, \mathbf{x}_{15}\}$. *The interface vertex* $\mathbf{x}_{12}$ *is a cross point. The first subdomain is* $\bar{\Omega}_1 = \{\mathbf{x}_1, \mathbf{x}_2, \mathbf{x}_9, \mathbf{x}_{10}, \mathbf{x}_{11}, \mathbf{x}_{12}\}$.

Throughout the present article, we will use (1.1) as a model problem. Nevertheless, we do not use any of the special features of (1.1) until section 3. For instance, our first main result (at the end of section 2) does not require that the matrix A be symmetric or positive definite.

2.1. Restriction matrices and traces. We now consider n-dimensional vectors. We interpret such a vector u as a function defined at each vertex $\mathbf{x}_j$. To each subdomain Ω_j, we may define a restriction matrix R_j, which restricts an arbitrary n-dimensional vector $\mathbf{u}$ to an n_j-dimensional vector $R_j\mathbf{u}$, which contains only the components of $\mathbf{u}$ corresponding to Ω_j and its artificial boundary $\partial\Omega_j \cap \Gamma$.

Example 2.1. The restriction matrix R_1 corresponding to Ω_1 in Figure 2.1 is

$$R_1 = \left[\begin{array}{cccccccccccccccc} \mathbf{1} & 0 & 0 & 0 & 0 & 0 & 0 & 0 & 0 & 0 & 0 & 0 & 0 & 0 & 0 & 0 \\ 0 & \mathbf{1} & 0 & 0 & 0 & 0 & 0 & 0 & 0 & 0 & 0 & 0 & 0 & 0 & 0 & 0 \\ \hline 0 & 0 & 0 & 0 & 0 & 0 & 0 & 0 & \mathbf{1} & 0 & 0 & 0 & 0 & 0 & 0 & 0 \\ 0 & 0 & 0 & 0 & 0 & 0 & 0 & 0 & 0 & \mathbf{1} & 0 & 0 & 0 & 0 & 0 & 0 \\ 0 & 0 & 0 & 0 & 0 & 0 & 0 & 0 & 0 & 0 & \mathbf{1} & 0 & 0 & 0 & 0 & 0 \\ 0 & 0 & 0 & 0 & 0 & 0 & 0 & 0 & 0 & 0 & 0 & \mathbf{1} & 0 & 0 & 0 & 0 \end{array}\right] = \left[\begin{array}{c} R_{I1} \\ \hline R_{\Gamma 1} \end{array}\right].$$

The top two rows, labeled R_{I1}, correspond to the restriction to the interior vertices $\{\mathbf{x}_1, \mathbf{x}_2\}$, while the bottom four rows, labeled $R_{\Gamma 1}$, correspond to the restriction to the interface vertices $\{\mathbf{x}_9, \mathbf{x}_{10}, \mathbf{x}_{11}, \mathbf{x}_{12}\}$.

We similarly partition $R_2, \ldots, R_p$ into interior parts R_{Ij} (top) and artificial interface parts $R_{\Gamma j}$ (bottom).

We further partition the finite element coefficient vector $\mathbf{u}_j$ so that the top part $\mathbf{u}_{Ij}$ corresponds to the vertices of $\Omega_j \setminus \Gamma$, while the bottom part $\mathbf{u}_{\Gamma j}$ corresponds to the vertices of $\partial\Omega_j \cap \Gamma$, i.e., $\mathbf{u}_j = \left[\begin{smallmatrix} \mathbf{u}_{Ij} \\ \mathbf{u}_{\Gamma j} \end{smallmatrix}\right]$. We can think of the vector $(\mathbf{u}_1^T, \ldots, \mathbf{u}_p^T)$ as a function which is defined on Ω, and which is continuous inside of each Ω_j, but which has jump discontinuities across Γ. For such a function, we define the multivalued or many-sided trace

$$\mathbf{u}_G = \left[\begin{array}{c} \mathbf{u}_{\Gamma 1} \\ \vdots \\ \mathbf{u}_{\Gamma p} \end{array}\right] \tag{2.1}$$

of dimension n_G. The n_G degrees of freedom of $\mathbf{u}_G$ correspond to vertices $\{\mathbf{x}_{n_I+1}, \ldots, \mathbf{x}_n\}$ on Γ, but $\mathbf{u}_G$ contains multiple degrees of freedom for each $\mathbf{x}_j$ (one per subdomain adjacent to $\mathbf{x}_j$). For each interface $\mathbf{x}_j \in \Gamma$, we let m_j be the number of subdomains adjacent to $\mathbf{x}_j$. We say that $\mathbf{x}_j$ is a regular interface vertex if $m_j = 2$, and we say that $\mathbf{x}_j$ is a cross point if $m_j \geq 3$.

The many-sided trace $\mathbf{u}_G$ has multiple function values per interface vertex $\mathbf{x} \in \Gamma$. If $\mathbf{u}$ is a (single-valued finite element) function on Ω, we may write $\mathbf{u} = \left[\begin{smallmatrix} \mathbf{u}_I \\ \mathbf{u}_\Gamma \end{smallmatrix}\right]$, where $\mathbf{u}_I$ corresponds to the points on $\Omega \setminus \Gamma$ and $\mathbf{u}_\Gamma$ corresponds to the points on Γ. Note that $\mathbf{u}_G$ is able to respresent functions disctontinuous across Γ and hence $\mathbf{u}_G$ has more degrees of freedom than $\mathbf{u}_\Gamma$.

2.2. Continuous many-sided traces. Although in general the many-sided trace $\mathbf{u}_G$ corresponds to a discontinuous function, it may happen that $\mathbf{u}_G$ corresponds in fact to a continuous function. This occurs precisely when the degrees of freedom of $\mathbf{u}_G$ associated with the interface vertices $\mathbf{x}_j$ all agree for each $j = n_I + 1, \ldots, n$. We now make this concept more explicit. To that end, we define $\breve{\Pi}$ to be the permutation matrix that reorders the entries of the many-sided trace $\mathbf{u}_G$ so that all degrees

of freedom associated with the first interface vertex $\mathbf{x}_{n_I+1}$ appear first, followed by the degrees of freedom associated with the second interface vertex $\mathbf{x}_{n_I+2}$, and so on. Then, for $k = n_I + 1, \dots, n$, we let

$$\check{M}_k = \begin{bmatrix} 1 & -\frac{1}{m_k-1} & \dots & -\frac{1}{m_k-1} \\ -\frac{1}{m_k-1} & 1 & \dots & -\frac{1}{m_k-1} \\ \vdots & \vdots & \ddots & \vdots \\ -\frac{1}{m_k-1} & -\frac{1}{m_k-1} & \dots & 1 \end{bmatrix} \in \mathbb{R}^{m_k \times m_k}. \tag{2.2}$$

Note that the kernel of $\check{M}_k$ is spanned by the vector of ones. Finally, let

$$M = \check{\Pi}^T \operatorname{diag}\{\check{M}_{n_I+1}, \dots, \check{M}_n\}\check{\Pi}. \tag{2.3}$$

By the construction of M, we have that $\mathbf{u}_G$ is a continuous many-sided trace if and only if

$$M\mathbf{u}_G = 0. \tag{2.4}$$

We also define the $n_G \times n_G$ symmetric matrix G of "interface interactions" by

$$G = \begin{bmatrix} R_{\Gamma 1}R_{\Gamma 1}^T & \dots & R_{\Gamma 1}R_{\Gamma p}^T \\ \vdots & \ddots & \vdots \\ R_{\Gamma p}R_{\Gamma 1}^T & \dots & R_{\Gamma p}R_{\Gamma p}^T \end{bmatrix}. \tag{2.5}$$

The entries of G are all either 0 or 1. The rows (or columns) of G precisely span the space of continuous many-sided traces, and hence we have that $MG = GM = 0$. The matrix $\check{\Pi}$ can be used to block-diagonalize G, and we obtain

$$G = \check{\Pi}^T \operatorname{diag}\{\mathbf{1}_{m_{n_I+1} \times m_{n_I+1}}, \dots, \mathbf{1}_{m_n \times m_n}\}\check{\Pi}, \tag{2.6}$$

where $\mathbf{1}_{m_j \times m_j}$ denotes the $m_j \times m_j$ matrix of ones.

We define the orthogonal projection matrix K (i.e., $K^2 = K$ and $K^T = K$) whose range is the space of continuous many-sided traces. It can be given succinctly using the matrix $\check{\Pi}$:

$$K = \check{\Pi}^T \operatorname{diag}\left\{\frac{1}{m_{n_I+1}}\mathbf{1}_{m_{n_I+1} \times m_{n_I+1}}, \dots, \frac{1}{m_n}\mathbf{1}_{m_n \times m_n}\right\}\check{\Pi}. \tag{2.7}$$

If $\mathbf{u}_1, \dots, \mathbf{u}_p$ are given and if the many-sided trace $\mathbf{u}_G$ is continuous, then there is a unique $\mathbf{u}$ such that

$$\mathbf{u}_k = R_k\mathbf{u}, \quad k = 1, \dots, p. \tag{2.8}$$

This $\mathbf{u}$ is given by "gluing together" the local functions $\mathbf{u}_1, \dots, \mathbf{u}_p$.

2.3. Decomposition of the matrix A. We now consider the $n \times n$ linear system (1.2), where A and $\mathbf{f}$ are given and $\mathbf{u}$ is the unknown quantity. We assume that the invertible "global stiffness matrix" A is decomposed into "local stiffness matrices" $A_{N1}, \dots, A_{Np}$, one per subdomain, and likewise for the data $\mathbf{f}$, such that

$$A = \sum_{j=1}^{p} R_j^T A_{Nj} R_j \quad \text{and} \quad \mathbf{f} = \sum_{j=1}^{p} R_j^T \mathbf{f}_j. \tag{2.9}$$

For $j = 1, \ldots, p$, the matrix A_{Nj} acts on the subdomain Ω_j and hence can be partitioned into blocks that act on the interior of Ω_j and on artificial interface vertices of Ω_j. We can likewise partition $\mathbf{f}_1, \ldots, \mathbf{f}_p$ to obtain

$$A_{Nj} = \begin{bmatrix} A_{IIj} & A_{I\Gamma j} \\ A_{\Gamma Ij} & A_{\Gamma\Gamma j} \end{bmatrix} \quad \text{and} \quad \mathbf{f}_j = \begin{bmatrix} \mathbf{f}_{I1} \\ \mathbf{f}_{\Gamma j} \end{bmatrix}.$$

In the case of the model problem (1.1), the local stiffness matrices correspond to problems with Neumann boundary conditions on the artificial interface, with bilinear forms

$$a_j(u, v) := \int_{\Omega_j} \nabla u \cdot \nabla v \quad \text{for } j = 1, \ldots, p, \tag{2.10}$$

where $u, v \in H_0^1(\Omega) \cap H^1(\Omega_j)$. The vector $\mathbf{f} = (f_j)$ is obtained from the functional $v \mapsto \int_{\Omega_j} fv$ using, e.g., the finite element method [35].

2.4. Robin subproblems. We multiply the PDE $-\Delta u_k = f$ in Ω_k by a test function ϕ and we integrate by parts to obtain the variational form $\int_{\Omega_k} \nabla u_k \cdot \nabla \phi - \int_{\partial\Omega_k \cap \Gamma} D_\nu u_k \phi$, where D_ν denotes the directional derivative in the direction of the outwards pointing normal ν of $\partial\Omega_k$. We assume we are given Robin data λ_k, and we use the equation $(a + D_\nu)u_k = \lambda_k$ on the artificial interface and discretize to obtain the following "local problems."

Given Robin data $\boldsymbol{\lambda}_1, \ldots, \boldsymbol{\lambda}_p$ and transmission condition matrices $B_1, \ldots, B_p$, we can compute "local solutions" $\mathbf{u}_1, \ldots, \mathbf{u}_p$ using

$$\begin{bmatrix} A_{IIk} & A_{I\Gamma k} \\ A_{\Gamma Ik} & A_{\Gamma\Gamma k} + B_k \end{bmatrix} \overbrace{\begin{bmatrix} \mathbf{u}_{Ik} \\ \mathbf{u}_{\Gamma k} \end{bmatrix}}^{\mathbf{u}_k} = \begin{bmatrix} \mathbf{f}_{Ik} \\ \mathbf{f}_{\Gamma k} + \boldsymbol{\lambda}_k \end{bmatrix} \text{ for } k = 1, \ldots, p. \tag{2.11}$$

We can eliminate interior nodes from (2.11) by using Schur complements. For each Neumann matrix A_{Nk}, we define the Schur complement and "condensed right-hand side"

$$S_k = A_{\Gamma\Gamma k} - A_{\Gamma Ik} A_{IIk}^{-1} A_{I\Gamma k} \quad \text{and} \quad \mathbf{g}_k = \mathbf{f}_{\Gamma k} - A_{\Gamma Ik} A_{IIk}^{-1} \mathbf{f}_{Ik}.$$

In order for these Schur complements to be well defined, we further assume that A_{IIk} is invertible for $k = 1, \ldots, p$. If A_{Nj} is obtained from (2.10), then A_{IIk} is automatically invertible (it is the stiffness matrix of a Dirichlet problem for Ω_k). We will further need to solve the Robin problems, and so we require that the matrices $S_k + B_k$ are nonsingular.

We define S and B to be the block-diagonal matrices $S = \operatorname{diag}\{S_1, \ldots, S_p\}$ and $B = \operatorname{diag}\{B_1, \ldots, B_p\}$, respectively, and we define $\mathbf{g}$ to be the column vector $\mathbf{g} = \left[\mathbf{g}_1^T, \ldots, \mathbf{g}_p^T\right]^T$. The system (2.11) is then equivalent to the Schur relation

$$(S + B)\mathbf{u}_G = \mathbf{g} + \boldsymbol{\lambda}. \tag{2.12}$$

In the domain decomposition parlance, the Schur complements $S_1, \ldots, S_p$ are known as (discrete) Dirichlet-to-Neumann maps. For the model problem (1.1), it is known that each S_j is nonsingular if $\partial\Omega_j$ intersects the natural boundary $\partial\Omega$. If $\partial\Omega_j$ does not intersect $\partial\Omega$, then the kernel of S_j is spanned by the vector $\mathbf{1}$ of ones. We then say that Ω_j floats. This characterization of the kernel of S will be used in section 3 and onward.

We also mention that each B_j is a mass matrix for the artificial interface $\partial\Omega_j \cap \Gamma$, and hence B_j is symmetric and positive definite. In particular, B_j and $S_j + B_j$ are invertible.

2.5. The equivalence of (1.2) and the 2LM method. In the present subsection, we show that the $n_G \times n_G$ system

$$A_{\mathrm{2LM}}\boldsymbol{\lambda} = \mathbf{h}, \tag{2.13}$$

where

$$A_{\mathrm{2LM}} = (BM - GB)(S+B)^{-1} + G \quad \text{and} \quad \mathbf{h} = -(BM - GB)(S+B)^{-1}\mathbf{g}, \tag{2.14}$$

is equivalent to (1.2). The solution $\boldsymbol{\lambda}$ of (2.13) is a many-sided trace $\boldsymbol{\lambda} = [\boldsymbol{\lambda}_1^T, \dots, \boldsymbol{\lambda}_p^T]^T$.

Our reasoning can be summarized as follows. Reasoning in terms of continuous functions, the Robin data λ is a linear combination of Dirichlet data u_G and "fluxes" $D_\nu u$. The fluxes should cancel in some suitable sense, and the Dirichlet data should be continuous. We see that averaging the Robin data (which are combinations of fluxes and Dirichlet data) ought to give something proportional to $\mathbf{u}_G$. Adapting this continuous reasoning to the discrete setting using the finite element discretization, we now describe the relationship between the Dirichlet and the Robin data.

LEMMA 2.2. *Assume that A is invertible. Let R_Γ be the matrix which restricts $\mathbf{u}$ to its single-valued trace $\mathbf{u}_\Gamma$: $R_\Gamma = \begin{bmatrix} 0 & I \end{bmatrix} \in \mathbb{R}^{(n-n_I)\times n}$. There is a unique solution $\mathbf{u}_1, \dots, \mathbf{u}_p, \boldsymbol{\lambda}_1, \dots, \boldsymbol{\lambda}_p$ to* (2.4), (2.11), *and*

$$\sum_k R_\Gamma R_{\Gamma k}^T \boldsymbol{\lambda}_k = \sum_k R_\Gamma R_{\Gamma k}^T B_k \mathbf{u}_{\Gamma k}. \tag{2.15}$$

Furthermore, the solution $\mathbf{u}$ to (2.8) *solves* (1.2).

Proof. Assume we have $\boldsymbol{\lambda}_1, \dots, \boldsymbol{\lambda}_p$ as well as $\mathbf{u}_1, \dots, \mathbf{u}_p$ satisfying (2.11), (2.4), (2.15). By (2.4), the local solutions $\mathbf{u}_1, \dots, \mathbf{u}_p$ meet continuously and we obtain a $\mathbf{u}$ such that (2.8) is satisfied. We see that, for this $\mathbf{u}$,

$$\begin{aligned} A\mathbf{u} &\overset{(2.9)}{=} \sum_k R_k^T \begin{bmatrix} A_{Ik} & A_{I\Gamma k} \\ A_{\Gamma I k} & A_{\Gamma\Gamma k} \end{bmatrix} R_k \mathbf{u} \\ &= \begin{bmatrix} A_{II}\mathbf{u}_I + A_{I\Gamma}\mathbf{u}_\Gamma \\ \sum_k R_\Gamma R_{\Gamma k}^T A_{\Gamma I k}\mathbf{u}_{Ik} + \sum_k R_\Gamma R_{\Gamma k}^T A_{\Gamma\Gamma k}\mathbf{u}_{\Gamma k} \end{bmatrix}, \end{aligned} \tag{2.16}$$

where we have used (2.8). Equation (2.11) further yields

$$A\mathbf{u} = \begin{bmatrix} \mathbf{f}_I \\ \mathbf{f}_\Gamma + \sum_k R_\Gamma R_{\Gamma k}^T \boldsymbol{\lambda}_k - \sum_k R_\Gamma R_{\Gamma k}^T B_k \mathbf{u}_{\Gamma k} \end{bmatrix} \overset{(2.15)}{=} \mathbf{f},$$

where we have partitioned the matrix $A = \left[\begin{smallmatrix} A_{II} & A_{I\Gamma} \\ A_{\Gamma I} & A_{\Gamma\Gamma} \end{smallmatrix}\right]$ into interior and interface (Γ) blocks. From (2.15), we see that any solution $\mathbf{u}_1, \dots, \mathbf{u}_p, \boldsymbol{\lambda}_1, \dots, \boldsymbol{\lambda}_p$ to the system (2.11), (2.4), (2.15) yields $\mathbf{u}$, via (2.8), which is the unique solution to $A\mathbf{u} = \mathbf{f}$, as required.

We now show the uniqueness of $\mathbf{u}_1, \dots, \mathbf{u}_p, \boldsymbol{\lambda}_1, \dots, \boldsymbol{\lambda}_p$. Assume that $\mathbf{u}_1^*, \dots, \mathbf{u}_p^*$, $\boldsymbol{\lambda}_1^*, \dots, \boldsymbol{\lambda}_p^*$ is a different solution of (2.11), (2.4), (2.15). If $\mathbf{u}_i = \mathbf{u}_i^*$ for $i = 1, \dots, p$, then (2.11) gives that $\boldsymbol{\lambda}_i = \boldsymbol{\lambda}_i^*$ for $i = 1, \dots, p$. Hence, we may assume that $\mathbf{u}_i \neq \mathbf{u}_i^*$ for some i. We then obtain $\mathbf{u}^*$ satisfying (2.8), for which again $A\mathbf{u}^* = \mathbf{f}$. Since A is

invertible, it must be that $\mathbf{u}^* = \mathbf{u}$. Hence, $\mathbf{u}_i^* = R_i\mathbf{u}^* = R_i\mathbf{u} = \mathbf{u}_i$, which contradicts $\mathbf{u}_i^* \neq \mathbf{u}_i$. Hence, the solution to the system (2.11), (2.4), (2.15) is unique. ∎

Using (2.12), the systems (2.4) and (2.15) (with (2.11) having been eliminated) become

$$M(S+B)^{-1}\boldsymbol{\lambda} = -M(S+B)^{-1}\mathbf{g} \quad \text{and} \tag{2.17}$$

$$\sum_{k=1}^{p} R_\Gamma R_{\Gamma k}^T (I - B_k(S_k+B_k)^{-1})\boldsymbol{\lambda}_k = \sum_{k=1}^{p} R_\Gamma R_{\Gamma k}^T B_k(S_k+B_k)^{-1}\mathbf{g}_k, \tag{2.18}$$

respectively. Since M is a square matrix, the system (2.17) is already square and hence the system (2.17), (2.18) is rectangular (taller than it is wide). By construction, any solution $\boldsymbol{\lambda}_1, \ldots, \boldsymbol{\lambda}_p$ can be turned into a solution $\mathbf{u}$ of $A\mathbf{u} = \mathbf{f}$ using (2.11) and then (2.8). It is more convenient to solve a square nonsingular system. This is achieved by picking some matrices C_1 and C_2 and finding the system $C_1(2.17) + C_2(2.18)$. We now make the choices $C_1 = B$ and

$$C_2 = \begin{bmatrix} R_{\Gamma 1} R_\Gamma^T \\ \vdots \\ R_{\Gamma p} R_\Gamma^T \end{bmatrix}. \tag{2.19}$$

These choices C_1 and C_2 give (2.13) and (2.14). (See section 2.6 for some motivation for these choices of C_1 and C_2.) We are now able to show our first main result.

THEOREM 2.3. *Assume that A and $S+B$ are invertible and B^{-1} is positive definite. The system* (2.13) *is equivalent to solving* (1.2).

Proof. It suffices to show that the rows of the left-hand side of (2.17) and (2.18) lie in the linear span of the rows of (2.14). We begin by recovering the rows of (2.18).

We left-multiply A_{2LM} by GB^{-1}. By construction, the rows of G are continuous many-sided traces, and hence $GM = 0$. Therefore,

$$GB^{-1}A_{\text{2LM}} = GB^{-1}G(I - B(S+B)^{-1}). \tag{2.20}$$

We will now show that the range of $GB^{-1}G$ is precisely the range of G. This will allow us to recover (2.18) from the rows of (2.20).

Let $k = \operatorname{rank} G$. Since B^{-1} is positive definite, there is a real number $\alpha > 0$ such that $\mathbf{v}^T B^{-1}\mathbf{v} \geq \alpha \mathbf{v}^T\mathbf{v}$ for all vectors $\mathbf{v}$. Let U be a matrix such that GU has orthonormal columns. We get that

$$\mathbf{v}^T U^T GB^{-1}GU\mathbf{v} \geq \alpha \mathbf{v}^T U^T GGU\mathbf{v} = \alpha \mathbf{v}^T\mathbf{v} \text{ for any } \mathbf{v}.$$

Hence, $X = U^T GB^{-1}GU$ is positive definite. Since X is a $k \times k$ matrix, we get that the rank of X is k. But,

$$k = \operatorname{rank} X = \operatorname{rank} U^T GB^{-1}GU \leq \operatorname{rank} GB^{-1}G \leq k.$$

Hence, $\operatorname{rank} GB^{-1}G = k = \operatorname{rank} G$ and the range of $GB^{-1}G$ is the entire range of G.

Therefore, there is a matrix Y such that $YGB^{-1}G = G$. Left-multiplying (2.20) by Y, we obtain

$$YGB^{-1}A_{\text{2LM}} = G(I - B(S+B)^{-1}). \tag{2.21}$$

We can now recover (2.18) by selecting suitable rows of (2.21). We now show how to do this.

Note that each row of R_Γ coincides with some row of some $R_{\Gamma j}$. Therefore, there is a matrix V, which selects the appropriate rows of

$$G = \begin{bmatrix} R_{\Gamma 1} \\ \vdots \\ R_{\Gamma p} \end{bmatrix} \begin{bmatrix} R_{\Gamma 1}^T & \dots & R_{\Gamma p}^T \end{bmatrix},$$

such that $VG = R_\Gamma \begin{bmatrix} R_{\Gamma 1}^T & \dots & R_{\Gamma p}^T \end{bmatrix}$. For this matrix V, we have

$$VYGB^{-1}A_{2\mathrm{LM}} = R_\Gamma \begin{bmatrix} R_{\Gamma 1}^T & \dots & R_{\Gamma p}^T \end{bmatrix} (I - B(S+B)^{-1}),$$

which is the matrix on the left-hand side of (2.18).

Now that we have recovered the matrix on the left-hand side of (2.18), we may recover (2.17) via the relation (2.13) $= C_1(2.17) + C_2(2.18)$, as required. ∎

Remark 2.4. For Theorem 2.3, we have not assumed that A is symmetric nor positive definite.

2.6. Motivation for the 2LM method. When the subdomains are arranged in a strip (and there are no cross points), it is known [36] that the Richardson iteration applied to (2.13) is equivalent to the OSM. This is interesting because the convergence properties of OSM [27] for special domains using Fourier transforms suggest that the condition number of $A_{2\mathrm{LM}}$ varies in the grid parameter h like $O(h^{-\frac{1}{2}})$. The remainder of the present article will show that this is true in general (cf. (4.3)) and will further elucidate the dependence of the condition number on the number of subdomains.

The choice of $C_1 = B$ and C_2 given by (2.19) was arrived at in the following way. We were aware of the relationship between OSM and 2LM for simple cases, which was shown in [36]. We looked for simple combinations of the matrices at hand, e.g., B, R_j, etc., which would generalize the example of [36], and this choice of C_1, C_2 achieves our objective.

3. The symmetric and positive definite case; condition number estimates. Assume that A is symmetric and positive definite and S is symmetric and semidefinite, and that the kernel of S is spanned by the indicator functions of the subdomains that float. (We will recapitulate all such assumptions in Definition 3.8.)

From (2.2), (2.6), (2.7), we see that $(M-G)K = MK - GK = -G$. Since the range of G is precisely the kernel of M, we also conclude that $M - G$ is invertible. Hence,

$$(M-G)^{-1}G = -K. \tag{3.1}$$

Therefore, we take $B = aI$ (where $a > 0$ is a parameter to be chosen) and we left-multiply (2.13) by $(M-G)^{-1}$ to obtain an equivalent symmetric system:

$$A_{\mathrm{S2LM}}\boldsymbol{\lambda} = \mathbf{h}_S, \text{ where } A_{\mathrm{S2LM}} = \overbrace{a(S+aI)^{-1}}^{Q} - K \text{ and } \mathbf{h}_S = -\overbrace{a(S+aI)^{-1}}^{Q}\mathbf{g}. \tag{3.2}$$

The matrix Q is interpreted as the Robin-to-Dirichlet map, scaled by the tuning parameter a. Since condition numbers are submultiplicative,

$$\mathcal{K}(A_{2\mathrm{LM}}) \le M_0\mathcal{K}(A_{\mathrm{S2LM}}) \text{ and } \mathcal{K}(A_{\mathrm{S2LM}}) \le M_0\mathcal{K}(A_{2\mathrm{LM}}), \tag{3.3}$$

where $M_0 = \mathcal{K}(M-G)$ and where $\mathcal{K}$ denotes the spectral condition number (the ratio of the largest to smallest singular values). We say that $A_{2\mathrm{LM}}$ and A_{S2LM} are spectrally equivalent. (We will see in section 3.1 that, under some conditions, M_0 is not too large.)

In order to estimate the condition number of A_{S2LM}, we prove a matrix analytical result which allows us to bound the modulus of the eigenvalues of A_{S2LM} below and above. We will make repeated use of the weighted Young inequality

$$|\xi\zeta| \le \frac{s}{2}\xi^2 + \frac{1}{2s}\zeta^2. \tag{3.4}$$

DEFINITION 3.1 (splitting of A_{S2LM}). *Let Q be a symmetric and positive definite matrix with eigenvalues $0 < q_1 \le q_2 \le \cdots \le q_n \le 1$. Let K be an orthogonal projection and define*

$$A_{\mathrm{S2LM}} = Q - K. \tag{3.5}$$

Let $P = I - Q$ and denote the k nonzero eigenvalues of P by $1 > p_1 \ge p_2 \ge \cdots \ge p_k > 0$. Let $\mathcal{N} = \ker P$ be the nullspace of P. Define E to be the orthogonal projection onto $\mathcal{N}$.

LEMMA 3.2. *Assume we have a splitting of A_{S2LM} as per Definition 3.1. Assume that there is a real number $0 \le r < 1$ such that*

$$\|E\mathbf{c}\| \le r\|\mathbf{c}\| \tag{3.6}$$

for every $\mathbf{c}$ such that $K\mathbf{c} = \mathbf{c}$, where $\|\cdot\|$ denotes the Euclidian norm. Assume that $0 < \min\{q_1, p_k\} < 0.5$ is and $0.5 < r < 1$. Then, the spectrum of $A_{\mathrm{S2LM}} = Q - K$ satisfies

$$|\sigma(A_{\mathrm{S2LM}})| \subset [\min\{p_k, q_1\}(1-r), 1]. \tag{3.7}$$

In particular, the condition number $\mathcal{K}(A_{\mathrm{S2LM}})$ is bounded by

$$\mathcal{K}(A_{\mathrm{S2LM}}) \le (\min\{p_k, q_1\}(1-r))^{-1}. \tag{3.8}$$

The proof of Lemma 3.2 is highly technical and can be found in the appendix.

We now give an example that shows that, for our purpose, (3.7) cannot be improved meaningfully without additional assumptions on A_{S2LM}.

Example 3.3 ($\sigma_{\min}(A_{\mathrm{S2LM}})$ with $n = 2$). For given parameters $\theta \in \mathbb{R}$ and $0 < q_1 < 1$, we set

$$K = \begin{bmatrix} \cos\theta \\ \sin\theta \end{bmatrix} \begin{bmatrix} \cos\theta & \sin\theta \end{bmatrix} = \begin{bmatrix} \cos^2\theta & \cos\theta\sin\theta \\ \cos\theta\sin\theta & \sin^2\theta \end{bmatrix},$$

$$Q = \begin{bmatrix} q_1 & \\ & 1 \end{bmatrix} \quad \text{and} \quad A_{\mathrm{S2LM}} = Q - K = \begin{bmatrix} q_1 - \cos^2\theta & -\cos\theta\sin\theta \\ -\cos\theta\sin\theta & \cos^2\theta \end{bmatrix}.$$

Note that we have chosen $n = 2$ and $k = 1$, and we have that $p_k = p_1 = 1 - q_1$. We then have that $r = \sin\theta$, or $\theta = \arcsin r$. Direct calculations give

$$\sigma_{\min}(A_{\mathrm{S2LM}}) = \frac{(p_k - 1) + \sqrt{(p_k+1)^2 - 4r^2 p_k}}{2}, \tag{3.9}$$

from which we find

$$1 \le \frac{\sigma_{\min}(A_{\mathrm{S2LM}})}{p_k(1-r)} \le 4 \quad \text{for all} \quad 0 < p_k < \frac{1}{2} \quad \text{and} \quad 0 < r < 1. \tag{3.10}$$

A series expansion further shows that $\sigma_{\min}(A_{\mathrm{S2LM}}) \approx 2p_k(1-r)$ near $p_k = 0$ and $r = 1$.

In dimensions $n \ge 3$, one can find examples of Q and K such that the condition number $\mathcal{K}(Q-K)$ is much smaller than $(p_k(1-r))^{-1}$, but Example 3.3 shows that the estimate (3.8) cannot be improved without further assumptions on A_{S2LM}.

3.1. Domain decomposition of radius ℓ. Since $\mathbf{c}$ is in the range of K, we interpret r as the spectral norm $\|EK\|$ of EK. Hence, we are looking for the square root of the spectral radius of EKE. This can be easily computed by choosing a matrix J whose columns form an orthonormal basis for the range of E, and we get that

$$r = \|J^T K J\|^{\frac{1}{2}}.$$

The range of E consists of piecewise constant many-sided traces, and hence we take

$$\tilde{J} = \begin{bmatrix} \frac{\mathbf{1}_{m_{\Gamma 1}}}{\sqrt{m_{\Gamma 1}}} & & \\ & \ddots & \\ & & \frac{\mathbf{1}_{m_{\Gamma 2}}}{\sqrt{m_{\Gamma 2}}} \\ 0 & \dots & 0 \\ \vdots & \ddots & \vdots \\ 0 & \dots & 0 \end{bmatrix}, \tag{3.11}$$

where $m_{\Gamma 1}$ is the number of vertices on $\partial\Omega_i$ for each floating subdomain. Since the kernel of E is zero on the natural boundary, we construct J by deleting those columns of $\tilde{J}$ corresponding to nonfloating subdomains.

LEMMA 3.4. *For $i \neq j$, we have*

$$(I - \tilde{J}^T K \tilde{J})_{ij} = -\frac{\#\{\mathbf{x}_k \in \partial\Omega_i \cap \partial\Omega_j\}}{\sqrt{m_{\Gamma i} m_{\Gamma j}}}. \tag{3.12}$$

Furthermore, the row sums of $I - \tilde{J}^T K \tilde{J}$ are zero.

Proof. We begin by showing that the rows sums of $I - \tilde{J}^T K \tilde{J} \in \mathbb{R}^{k \times k}$ are zero. Let $e_k \in \mathbb{R}^k$ be the column vectors of ones. From (3.11) we see that $Je_k = e_n \in \mathbb{R}^n$ is the n-dimensional vector of ones. Regarded as a multivalued trace, the constant vector e_n of ones is continuous, and hence $Ke_n = e_n$. As a result, $(I - \tilde{J}^T K \tilde{J})e_k = e_k - \tilde{J}^T K e_n = e_k - \tilde{J}^T e_n = e_k - e_k = 0$, and hence the row sums of $I - \tilde{J}^T K \tilde{J}$ are zero, as required.

We now compute the off-diagonal entries of $I - \tilde{J}^T K \tilde{J}$. For $i \neq j$, we find that

$$(I - \tilde{J}^T K \tilde{J})_{ij} = -e_i^T \tilde{J}^T K \tilde{J} e_j = -(K\tilde{J}e_i)^T (K\tilde{J}e_j),$$

where e_i and e_j are the usual canonical basis vectors of $\mathbb{R}^k$. Note that $\tilde{J}e_j$ is simply the jth column of $\tilde{J}$, which is a function whose value is the constant $1/\sqrt{m_{\Gamma j}}$ on Ω_j. Multiplying this function by K produces a continuous multivalued trace whose value at vertex $\mathbf{x}_k \in \partial\Omega_j$ is $\frac{1}{m_k \sqrt{m_{\Gamma j}}}$, where m_k is the number of subdomains adjacent to $\mathbf{x}_k$, which gives (3.12). ∎

Lemma 3.4 states that $I - \tilde{J}^T K \tilde{J}$ is a topological Laplacian for the graph of the domain decomposition, with weights on the edges corresponding to the number of vertices on the artificial interfaces of the subdomains. Because the row sums are zero, this topological Laplacian has Neumann boundary conditions. Thus, matrix $I - J^T K J$, which is obtained by deleting rows and columns of $I - \tilde{J}^T K \tilde{J}$ corresponding to nonfloating subdomains, is a topological Laplacian with homogeneous Dirichlet conditions on the nonfloating subdomains. We not estimate the smallest eigenvalue of this topological Laplacian.

DEFINITION 3.5 ((a,b,ℓ) path decomposition). *An L_1-path of length ℓ is a vector $\gamma = (i_1, i_2, \ldots, i_\ell) \in \{1,\ldots,p\}^\ell$ which describes a path $(\Omega_{i_1}, \Omega_{i_2}, \ldots, \Omega_{i_\ell})$ of adjacent subdomains, such that $\Omega_2, \ldots, \Omega_\ell$ all float but Ω_1 is a nonfloating subdomain and such that*

$$L_1 \leq \frac{\#\{\mathbf{x}_k \in \partial\Omega_{i_{j-1}} \cap \partial\Omega_{i_j}\}}{\sqrt{m_{\Gamma i_{j-1}} m_{\Gamma i_j}}} \text{ for } i = 2, \ldots, \ell.$$

An (L_1, ℓ) path decomposition $(\gamma_1, \ldots, \gamma_q)$ is a partition of the domain decomposition $\Omega_1, \ldots, \Omega_p$ into disjoint paths $\{\gamma_k\}$, each of which is an L_1-path of length at most ℓ.

LEMMA 3.6. *Assume that the domain decomposition admits an (a,b,ℓ) path decomposition. Then,*

$$r \leq 1 - \frac{L_1 \pi^2}{2\ell^2}. \tag{3.13}$$

Proof. We write the path decomposition as $\gamma_1, \ldots, \gamma_q$ with $\gamma_k = (\gamma_{k1}, \ldots, \gamma_{k\ell_k})$ and $\ell_k \leq \ell$ for every k. The path decomposition allows us to write $\sum_{k=1}^q X_q \preceq I - \tilde{J}^T K \tilde{J}$, where each matrix X_k is given by the symmetric and semidefinite matrix given by

$$X_k = L_1 \begin{bmatrix} 1 & -1 & & & \\ -1 & 2 & -1 & & \\ & -1 & 2 & -1 & \\ & & \ddots & \ddots & \ddots \\ & & & -1 & 2 \end{bmatrix} \in \mathbb{R}^{\ell_k \times \ell_k},$$

where ℓ_k is the length of the path γ_k. The smallest eigenvalue of $I - J^T K J$ is estimated by considering the Rayleigh quotient $u^T(I - \tilde{J}^T K \tilde{J})u$, where u is restricted to be zero on the natural boundary. Hence,

$$\lambda_{\min}(I - \tilde{J}^T K \tilde{J}) \geq \min_{u=0 \text{ on } \partial\Omega} \sum_{k=1}^q \frac{u^T X_k u}{u^T u}.$$

We have that

$$\begin{aligned} u^T X_k u &= L_1 \begin{bmatrix} 0 & u_{\gamma_{k2}} & \ldots & u_{\gamma_{k\ell_k}} \end{bmatrix} \begin{bmatrix} 1 & -1 & & & & \\ -1 & 2 & -1 & & & \\ & -1 & 2 & -1 & & \\ & & \ddots & \ddots & \ddots & \\ & & & -1 & 2 \end{bmatrix} \begin{bmatrix} 0 \\ u_{\gamma_{k2}} \\ \vdots \\ u_{\gamma_{k\ell_k}} \end{bmatrix} \\ &= L_1 \begin{bmatrix} u_{\gamma_{k2}} & \ldots & u_{\gamma_{k\ell_k}} \end{bmatrix} \begin{bmatrix} 2 & -1 & & \\ -1 & 2 & -1 & \\ & \ddots & \ddots & \ddots \\ & & -1 & 2 \end{bmatrix} \begin{bmatrix} u_{\gamma_{k2}} \\ \vdots \\ u_{\gamma_{k\ell_k}} \end{bmatrix} \\ &\geq L_1(2 - 2\cos(\pi/(\ell_k+1))) \sum_{j=1}^{\ell_k} u^2_{\gamma_{k\ell_k}}. \end{aligned}$$

Because each j is in some path of length $\ell_k \leq \ell$, we obtain

$$\lambda_{\min}(I - \tilde{J}^T K \tilde{J}) \geq L_1(2 - 2\cos(\pi/\ell)).$$

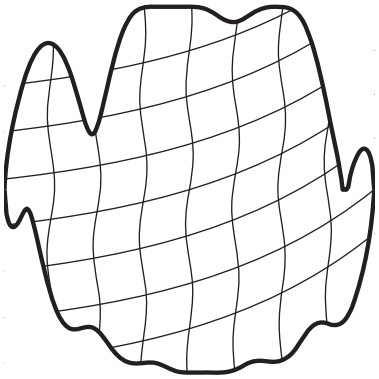

FIG. 3.1. *A domain decomposition with* $\ell = 4$.

Hence,

$$r = \|J^T K J\|^{1/2} \leq (1 - L_1(2 - 2\cos(\pi/(\ell+1))))^{1/2} \leq 1 - \frac{L_1 \pi^2}{2\ell^2},$$

as required. ∎

Remark 3.7. In a typical situation where Ω has unit diameter and all the subdomains are approximately the same size, the Euclidian diameter H of the subdomains is roughly $1/\ell$. If the coarse grid has some regularity (e.g., edges and faces separating subdomains all have comparable number of vertices), then L_1 is also bounded away from 0. An example of such a domain decomposition is displayed in Figure 3.1. Furthermore, from (2.2) and (2.6) one finds that $M_0 = \max_k m_k - 1$, which is only large in degenerate cases where grid vertices have large degrees.

3.2. Condition numbers of A_{2LM} and A_{S2LM}. Our second main result is algebraic.

DEFINITION 3.8 (regular algebraic domain decomposition). *We say that an algebraic domain decomposition is regular if the following properties hold. Assume that A is symmetric and positive definite. We let Ω be a domain and $\Omega_1, \ldots, \Omega_p$ be a domain decomposition with restriction matrices $R_1, \ldots, R_p$. We assume that S is symmetric and semidefinite and that the kernel of S is spanned by the indicator functions of the subdomains that float. We let $s_{\min} > 0$ be the smallest* nonzero *eigenvalue of S, and $s_{\max}$ be the largest eigenvalue of S with "nonsingular" condition number $\mathcal{K}_0(S) = \frac{s_{\max}}{s_{\min}}$. We let $B = a_{\mathrm{opt}} I$, where*

$$a_{\mathrm{opt}} = \sqrt{s_{\max} s_{\min}}. \tag{3.14}$$

We define K by (2.7) *and A_{S2LM} by* (3.2). *We define M by* (2.3), *G by* (2.6), *and A_{2LM} by* (2.14). *We assume that the domain decomposition is has an (L_1, ℓ) path decomposition.*

THEOREM 3.9 (condition number estimates for A_{2LM} and A_{S2LM}, algebraic case). *Assume that we are given a regular algebraic domain decomposition:*

$$\mathcal{K}(A_{\mathrm{S2LM}}) \leq 2\, \frac{\left(1 + \sqrt{\mathcal{K}_0(S)}\right) \ell^2}{L_1\, \pi^2}. \tag{3.15}$$

Proof. We let $Q = a(S + aI)^{-1}$ (cf. (3.2)) with eigenvalues $0 < q_1 \leq \cdots \leq q_n \leq 1$ and $P = I - Q = S(S + aI)^{-1}$ with positive eigenvalues $1 > p_1 \geq \cdots \geq p_k > 0$, as per the statement of Lemma 3.2. We calculate that

$$p_k = \min_{z \in \{s_{\min}, \ldots, s_{\max}\}} \frac{z}{z + a_{\text{opt}}} = \frac{s_{\min}}{s_{\min} + \sqrt{s_{\min} s_{\max}}} = \frac{1}{1 + \sqrt{\mathcal{K}_0(S)}} \quad \text{and} \tag{3.16}$$

$$q_1 = \min_{z \in \{0, s_{\min}, \ldots, s_{\max}\}} \frac{a_{\text{opt}}}{z + a_{\text{opt}}} = \frac{\sqrt{s_{\min} s_{\max}}}{s_{\max} + \sqrt{s_{\min} s_{\max}}} = \frac{1}{1 + \sqrt{\mathcal{K}_0(S)}} = p_k. \tag{3.17}$$

We substitute the value of r given by (3.13), and the values of p_k and q_1 into (3.8) yield (3.15). ∎

4. Estimates for the elliptic case. The main application is for elliptic problems.

DEFINITION 4.1 (regular geometric domain decomposition). *We have a regular geometric domain decomposition when the following properties hold. Let $h > 0$ be the fine grid parameter, and let $H > 0$ be the typical subdomain size. Let Ω be a domain of unit diameter. We assume all the hypotheses of a regular algebraic domain decomposition. In addition, we assume the following:*

1. *$\Omega_1, \ldots, \Omega_p$ are polygons or polyhedra of diameter $H_i < H$.*
2. *For $i = 1, \ldots, p$, either Ω_i floats or the size of the intersection of $\partial\Omega_i$ with $\partial\Omega$ is comparable to $\partial\Omega_i$.*
3. *The triangulation T_h is* quasi-uniform *(cf.* [37, Definition B.3]*).*
4. *The matrix A is the finite element discretization of the bilinear form*

$$a(u, v) = \int_\Omega a(\mathbf{x}) \nabla u(\mathbf{x}) \cdot \nabla v(\mathbf{x})\, d\mathbf{x}$$

with piecewise polynomial basis functions. The function $a(\mathbf{x})$ is assumed to be bounded $0 < a_{\min} \leq a(\mathbf{x}) \leq a_{\max}$ in such a way that $a(u, v)$ is equivalent to the seminorm $\int_\Omega \nabla u \cdot \nabla v$. We further assume that $a(\mathbf{x})$ is constant on each subdomain Ω_i.

We begin by formulating a standard estimate in a form which is suitable for our use.

LEMMA 4.2. *Assume that we have a regular geometric domain decomposition. There is a constant C_{dd}, which depends on the shape of Ω and the subdomains, but not on the grid parameter h or on the size of the subdomains, such that the inequality*

$$\mathcal{K}_0(S) \leq C_{dd} \frac{H}{h} \tag{4.1}$$

is satisfied.

Proof. By replacing each subdomain Ω_i by $\frac{1}{H_i}\Omega_i$, we may assume without loss of generality that $H_i = 1$. Let $\mathbf{u}_{\Gamma i}$ be a (finite element) trace on $\partial\Omega_i$. If Ω_i floats, further assume that the average of $\mathbf{u}_{\Gamma i}$ is zero (so that $\mathbf{u}_{\Gamma i}$ is orthogonal to the kernel of S_i). According to [37, Lemma 4.10], there are constants c and C such that

$$c |\mathbf{u}_{\Gamma i}|^2_{H^{\frac{1}{2}}(\partial\Omega_i)} \leq \mathbf{u}_i^T S_i \mathbf{u}_i \leq C |\mathbf{u}_{\Gamma i}|^2_{H^{\frac{1}{2}}(\partial\Omega_i)}. \tag{4.2}$$

According to [37], all constants appearing in the present proof depend on the regularity and shape of the domain decomposition and on the elliptic operator, but do not depend on the size or number of the subdomains, or on the finite element grid parameter h.

There is also a constant c' such that $\|\mathbf{u}_{\Gamma i}\|_{L^2(\partial\Omega_i)} \leq c'|\mathbf{u}_{\Gamma i}|_{H^{\frac{1}{2}}(\partial\Omega_i)}$ [37, Lemma A.17]. There is yet another constant C' such that $|\mathbf{u}_{\Gamma i}|_{H^{\frac{1}{2}}(\partial\Omega_i)} \leq \frac{C'}{\sqrt{h}}\|\mathbf{u}_{\Gamma i}\|_{L^2(\partial\Omega_i)}$ [37, Lemma B.5]. Hence, the estimate (4.2) becomes

$$\frac{c}{(c')^2}\|\mathbf{u}_{\Gamma i}\|^2_{L^2(\partial\Omega_i)} \leq \mathbf{u}_i^T S_i \mathbf{u}_i \leq \frac{C(C')^2}{h}\|\mathbf{u}_{\Gamma i}\|^2_{L^2(\partial\Omega_i)}.$$

The spectral equivalence of $\mathbf{u}_{\Gamma i}^T\mathbf{u}_{\Gamma i}$ and $\|\mathbf{u}_{\Gamma i}\|^2_{L^2(\partial\Omega_i)}$ [37, Lemma B.5 or the end of the proof of Lemma 4.11] gives (4.1). ∎

Our third main result is the condition number estimates for the 2LM method for an elliptic problem.

THEOREM 4.3 (condition number estimates for A_{2LM} and A_{S2LM} for elliptic PDEs). *Assume that we have a regular geometric domain decomposition. When h and H are sufficiently small, the condition numbers $\mathcal{K}(A_{\text{S2LM}})$ and $\mathcal{K}(A_{\text{2LM}})$ are bounded by*

$$\mathcal{K}(A_{\text{S2LM}}), \mathcal{K}(A_{\text{2LM}}) \leq CH^{-\frac{3}{2}}h^{-\frac{1}{2}}, \tag{4.3}$$

where the constant C depends on the regularity of the elliptic form $a(u,v)$ as well as the shape of Ω and the shapes of the subdomains, but not on the sizes or number of subdomains, nor on the parameter h of the triangulation T_h.

The proof is by substituting the estimate (4.1) into the condition number estimates of Theorem 3.9.

4.1. Remarks on Krylov space methods. The 2LM methods are linear problems that must be solved, and it is natural to use a Krylov space solver. We now briefly summarize the convergence theory for GMRES and refer to [7] and references therein for details.

The matrix A_{S2LM} is symmetric and indefinite. For such matrices, the condition number provides a linear convergence bound for GMRES, and the asymptotic convergence factor is

$$\frac{\mathcal{K}-1}{\mathcal{K}+1} < 1. \tag{4.4}$$

For symmetric and indefinite matrices, the minimum residual algorithm MINRES is mathematically equivalent to GMRES and has a two-term recurrence, although the numerical issues surrounding the loss of orthogonality signify that MINRES and GMRES perform differently in practice.

Because our condition number is $\mathcal{K} = O(h^{-\frac{1}{2}}H^{-\frac{3}{2}})$, if we consider purely the condition numbers, we find that our new methods are expected to scale better than classical Schwarz methods in the h variable alone. However, a 1-level Schwarz algorithm scales like $O(h^{-1}H^{-1})$, and so there is better scaling in the H variable and it has the added benefit of being easy to implement, since it corresponds to the block-Jacobi preconditioned.

However, within the context of a Krylov space solver, an additive Schwarz preconditioner is symmetric and positive definite and hence benefits from a "free" square root in its performance for GMRES or CG. Therefore, for A_{S2LM}, we expect an overall scaling in performance in the h variable to be roughly comparable to an additive Schwarz preconditioner, and there is no special benefit in using one method over the other—both the additive Schwarz method and the A_{S2LM} method can be used with Krylov space solvers that have short recurrences (CG and MINRES, respectively).

The matrix A_{2LM} is nonsymmetric, and as a result, the condition number is not necessarily related to the performance of GMRES. Actual convergence bounds for nonsymmetric matrices can be obtained from the field of values and from resolvent norm estimates. The latter is the subject of the upcoming paper [8].

The nonsymmetric method A_{2LM} may indeed produce an overall algorithm which scales better than additive Schwarz when used in combination with GMRES (or CG for additive Schwarz). This good scaling behavior is not revealed by our analysis of condition numbers alone, but the numerical experiments in section 5.2 suggest that indeed the algorithm GMRES on A_{2LM} scales very well. This apparent improved scaling comes at a cost, since GMRES does not have a short recurrence.

We mention one advantage of our methods. Our local problems have better condition numbers since $\mathcal{K}(Q) = \sqrt{\mathcal{K}_0(S)}$. This may be beneficial if the local problems are solved iteratively.

5. Numerical experiments. We offer two sets of experiments. In the first set, we confirm the condition number estimate (4.3). In the second set of experiments, we investigate the behavior of GMRES on the matrices A_{2LM} and A_{S2LM}.

5.1. Verifying the condition number estimate (4.3). We confirm the estimate (4.3) with numerical experiments which we now describe. We verify the scaling of the condition number of A_{S2LM}, as measured with the `eigs` command of MATLAB, in the parameters ℓ and in h for the usual 5-point discrete Laplacian on the unit square with a regular grid and with homogeneous Dirichlet data. Subdomains are arranged as a grid of size ℓ, normalized to the unit square.

In Figure 5.1 (left), we use 3×3 subdomains ($\ell = 2$ and 4 cross points) and vary the value of the finite element grid parameter $h = \frac{1}{7}, \frac{1}{15}, \frac{1}{31}, \frac{1}{63}, \frac{1}{127}$. Our experiments confirm the scaling behavior $(4.3) = O(h^{-\frac{1}{2}})$.

In Figure 5.1 (right), we take subdomains of width $H = \frac{1}{\ell+1}$ and $h = \frac{H}{5}$ and we vary the diameter $\ell = 2, 4, 8, 16$ (up to $17 \times 17 = 289$ subdomains and 256 cross points). Our experiments confirm the scaling behavior $(4.3) = O(H^{-2})$.

5.2. Experiments with GMRES. We now perform a scaling experiment with GMRES on A_{S2LM} and A_{2LM}. We use 4×4 subdomains and vary h. We then run GMRES until the relative residual drops below 10^{-6}. For the initial residual, we use

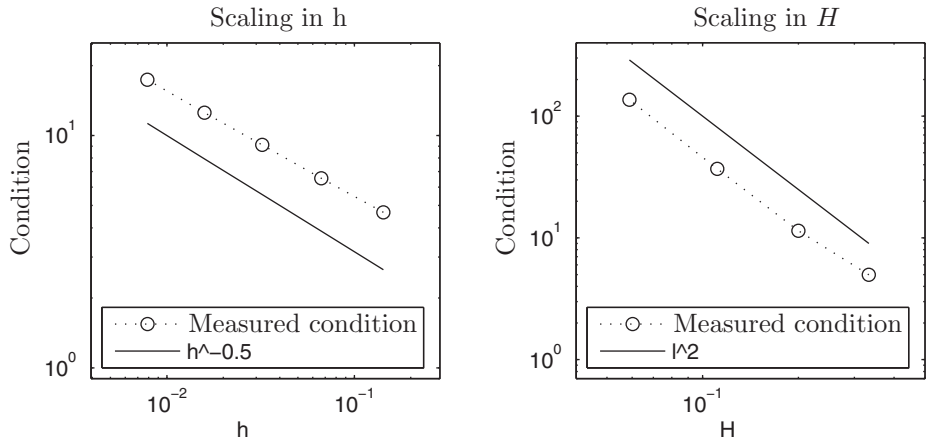

FIG. 5.1. *Scaling of the condition number. Left: as a function of h. Right: as a function of ℓ.*

TABLE 5.1
Number of GMRES iterations.

	A_{S2LM}	A_{2LM}	Schwarz
$h = 1/17$	22	16	50
$h = 1/33$	32	17	69
$h = 1/65$	49	19	86

a vector of ones. We report the number of iterations in Table 5.1. We thus confirm the estimated asymptotic convergence factor (4.4). Indeed, the predicted increase in iteration count going from $h = 1/33$ to $h = 1/65$ is roughly a factor of $\sqrt{2}$; the observed increase in iteration counts is a factor 1.5, which is in good agreement.

Since A_{2LM} is nonsymmetric, the iteration counts need not be related to the condition number of A_{2LM}. Nevertheless, we observe that the nonsymmetric matrix A_{2LM} performs much better than A_{S2LM}, both in terms of absolute iteration counts and in terms of scaling in the h variable.

For comparison, we also include iterations with the additive Schwarz preconditioner.

6. Conclusions. We have given a new optimized 2LM method and provided condition number estimates. Our new 2LM is a generalization of previous algorithms to the case where the domain and subdomains have cross points. The condition number estimates are consistent with the optimized Schwarz literature and are verified by numerical experiments.

7. Appendix. In this appendix, we give a sketch of the proof of Lemma 3.2. This proof is highly technical. The complete proof has several cases, according to which of p_k or q_1 is smaller, etc. The various cases are all similar to one another. Accordingly, we give a detailed proof for one case, and we summarize the other cases.

Sketch of proof of Lemma 3.2. The spectrum of Q can be given as a function of the spectrum of S:

$$\sigma(Q) = \left\{ \frac{a}{z+a} \quad : \quad z \in \sigma(S) \right\}.$$

Note that $0 < \frac{a}{z+a} \leq 1$ (since $z \geq 0$ by the semidefinite hypothesis on S) and hence $\sigma(Q) \subset [0,1]$. Since $\sigma(K) = \{0,1\}$, we have that $\sigma(A_{\mathrm{S2LM}}) = \sigma(Q-K) \subset [-1,1]$, which proves the upper bound of (3.7). We now estimate the eigenvalue of A_{S2LM} with the smallest magnitude.

For any given $\boldsymbol{\lambda}$, define $\mathbf{c} = K\boldsymbol{\lambda}$ (the continuous part of $\boldsymbol{\lambda}$) and $\mathbf{d} = \boldsymbol{\lambda} - \mathbf{c}$ (the discontinuous part of $\boldsymbol{\lambda}$). In this way, $\|\boldsymbol{\lambda}\|^2 = \|\mathbf{c}\|^2 + \|\mathbf{d}\|^2$ and $A_{\mathrm{S2LM}}\boldsymbol{\lambda} = -P\mathbf{c} + Q\mathbf{d}$. By the spectral theorem, without loss of generality we may assume that P and Q are both diagonal matrices $P = \mathrm{diag}\{p_1, \ldots, p_k, 0, \ldots, 0\}$ and $Q = \mathrm{diag}\{q_1, \ldots, q_k, 1, \ldots, 1\}$, since P and Q are symmetric and $PQ = QP$. Therefore, we have

$$\|A_{\mathrm{S2LM}}\boldsymbol{\lambda}\|^2 = \sum_{i=1}^{k} p_i^2 c_i^2 + \sum_{i=1}^{n} q_i^2 d_i^2 - 2\sum_{i=1}^{k} p_i c_i q_i d_i.$$

We introduce a parameter $t > 0$ (to be determined later) and use the hypothesis that

$\mathbf{c}^T\mathbf{d} = 0$ to obtain

$$\begin{aligned}\|A_{\mathrm{S2LM}}\boldsymbol{\lambda}\|^2 &= \sum_{i=1}^{k} p_i^2 c_i^2 + \sum_{i=1}^{n} q_i^2 d_i^2 - 2\sum_{i=1}^{k} p_i c_i q_i d_i + 2\sum_{i=1}^{n} t c_i d_i \\ &= \sum_{i=1}^{k} p_i^2 c_i^2 + \sum_{i=1}^{n} q_i^2 d_i^2 - 2\sum_{i=1}^{k} \left(1 - \frac{t}{p_i q_i}\right) p_i c_i q_i d_i + 2\sum_{i=k+1}^{n} t c_i d_i.\end{aligned}$$

We now use the weighted Young inequality (3.4) with the choices $\xi = p_i c_i$, $\zeta = q_i d_i$, and $s = s_i > 0$ for $i = 1, \ldots, k$, where we have introduced the positive parameters $s_1, \ldots, s_k$, which will be determined later. In addition, we also use the weighted Young inequality with the choices $\xi = c_i$, $\zeta = d_i$, and $s = \sigma$ for $i = k+1, \ldots, n$, where $\sigma > 0$ will be determined later. We obtain

$$\begin{aligned}\|A_{\mathrm{S2LM}}\boldsymbol{\lambda}\|^2 \geq{}& \sum_{i=1}^{k} p_i^2 \left(1 - \left(1 - \frac{t}{p_i q_i}\right) s_i\right) c_i^2 + \sum_{i=1}^{k} q_i^2 \left(1 - \left(1 - \frac{t}{p_i q_i}\right) s_i^{-1}\right) d_i^2 \\ &+ \sum_{i=k+1}^{n} (1 - t\sigma^{-1}) d_i^2 - \sum_{i=k+1}^{n} t\sigma c_i^2.\end{aligned}$$

Now we use the hypothesis that $\|E\mathbf{c}\| \leq r\|\mathbf{c}\|$, which implies that $\|E\mathbf{c}\|^2 \leq \frac{r^2}{1-r^2}\|(I - E)\mathbf{c}\|^2$, and hence

$$\begin{aligned}\|A_{\mathrm{S2LM}}\boldsymbol{\lambda}\|^2 \geq{}& \sum_{i=1}^{k} \overbrace{\left(p_i^2 - p_i^2 \left(1 - \frac{t}{p_i q_i}\right) s_i - \frac{t\sigma r^2}{1 - r^2}\right)}^{\alpha_i} c_i^2 \\ &+ \sum_{i=1}^{k} \overbrace{q_i^2 \left(1 - \left(1 - \frac{t}{p_i q_i}\right) s_i^{-1}\right)}^{\beta_i} d_i^2 + \sum_{i=k+1}^{n} (1 - t\sigma^{-1}) d_i^2 \\ &\geq \min_i\{\alpha_i\}\|(I - E)\mathbf{c}\|^2 + \min_i\{\beta_i\}\|(I - E)\mathbf{d}\|^2 + (1 - t\sigma^{-1})\|E\mathbf{d}\|^2.\end{aligned} \tag{7.1}$$

We again use that $\|E\mathbf{c}\| \leq r\|\mathbf{c}\|$, which implies that $\|(I - E)\mathbf{c}\|^2 \geq (1 - r^2)\|\mathbf{c}\|^2$, and hence

$$\|A_{\mathrm{S2LM}}\boldsymbol{\lambda}\|^2 \geq \overbrace{\min\left\{(1 - r^2)\min_i\{\alpha_i\}, \min_i\{\beta_i\}, 1 - t\sigma^{-1}\right\}}^{\rho} \|\boldsymbol{\lambda}\|^2.$$

There are now two cases to consider, namely, $\min\{p_k, q_1\} = p_k$ and $\min\{p_k, q_1\} = q_1$. We treat the case $\min\{p_k, q_1\} = p_k$ in detail; the case $\min\{p_k, q_1\} = q_1$ is done in a similar fashion.enlargethispage-12pt

We now choose the parameters $s_1, \ldots, s_k, \sigma, t$ in such a way that $\rho \geq p_k^2(1 - r)^2$. This can be achieved using the following procedure. First, we solve $1 - t\sigma^{-1} = p_k^2(1 - r)^2$ for t. Then we solve $\beta_i = p_k^2(1 - r)^2$ for s_i (cf. (7.1)). The resulting weights are

$$t = \sigma - \sigma\overbrace{(r - 1)^2 p_k^2}^{<1} > 0 \quad \text{and} \quad s_i = \frac{q_i\left(p_i q_i - \sigma + \sigma\,(r - 1)^2 {p_k}^2\right)}{p_i \underbrace{\left({q_i}^2 - {p_k}^2 (r - 1)^2\right)}_{>0}}. \tag{7.2}$$

The coefficient t is positive, and so is the coefficient s_i, provided that σ is small enough. We make the choice

$$\sigma = p_k(1-r) \tag{7.3}$$

and check (by substituting into (7.2)) that this value of σ is small enough so that s_i is indeed positive, provided $p_k < r$.

We substitute the values of t, s_i, q_i, and σ given by (7.2), (7.3), and $q_i = 1 - p_i$ into $(1-r^2)\alpha_i$ to obtain

(7.4)

$$\begin{aligned}\phi(p_i) &:= (1-r^2)\alpha_i \\ &= \Big((-1+r)\, p_k \Big(-2\, p_i\, (-1+r)\, (r+1)\, (-1+p_i) - (-1+r)^5\, {p_k}^5 \\ &\quad - (-1+r)\left(-2\, p_i r^2 + 1 + {p_i}^2\right) p_k + 2\, p_i\, (r+1)\, (-1+r)^3\, (-1+p_i)\, {p_k}^2 \\ &\quad + (-1+r)^3 \left(-2\, p_i r^2 + {p_i}^2 r^2 + 2\right) {p_k}^3 \Big) \Big) \Big/ \Big((-1+p_i)^2 - {p_k}^2\, (-1+r)^2 \Big).\end{aligned}$$

The function $\phi(p_i)$ has no singularities in the interval $p_i \in [p_k, 1-p_k]$ and $\phi'(p_i) = 0$ at the roots

$$p^{(1)} = \frac{-1 + {p_k}^2\, (-1+r)^2}{-1 + (-1+r)\, p_k + {p_k}^2\, (-1+r)^2} \quad \text{and} \tag{7.5}$$

$$p^{(2)} = -\left(p_k r - p_k - 1\right) \left(p_k r - p_k + 1\right)^2. \tag{7.6}$$

We now find the sign of $\Phi_{p_i}(r, p_k) := \phi(p_i) - p_k^2 (1-r)^2$. Since $\phi(p_i)$ is a differentiable function for $p_i \in [p_k, 1-p_k]$, we have that

$$\Phi_{p_i}(r, p_k) \geq \min_{p_i \in \{p^{(1)}, p^{(2)}, p_k, 1-p_k\}} \Phi_{p_i}(r, p_k).$$

We consider the case $p^{(1)}$ in detail, and the other cases are similar.

To find the sign of $\Phi_{p^{(1)}}(r, p_k)$, we solve $\Phi_{p^{(1)}}(r, p_k) = 0$ for the unknown p_k, giving the roots

$$p_k^{1,\pm} = \pm \frac{\sqrt{1-r^2}}{r-1} \quad \text{and} \quad p_k^{2,\pm} = \frac{\pm 1}{r-1}.$$

We have plotted these roots in the (r, p_k) plane in Figure 7.1 (top-left). We note that the zeros of $\Phi_{p^{(1)}}(r, p_k)$ (as a function of p_k and r) do not intersect the rectangle $R = \{(r, p_k) \mid 0.204 < r < 1 \text{ and } 0 < p_k < 0.5\}$. We then compute $\Phi_{p^{(1)}}(0.5, 0.25) \approx 0.7229 > 0$, which proves that $\Phi_{p^{(1)}}(r, p_k)$ is positive throughout the rectangle R.

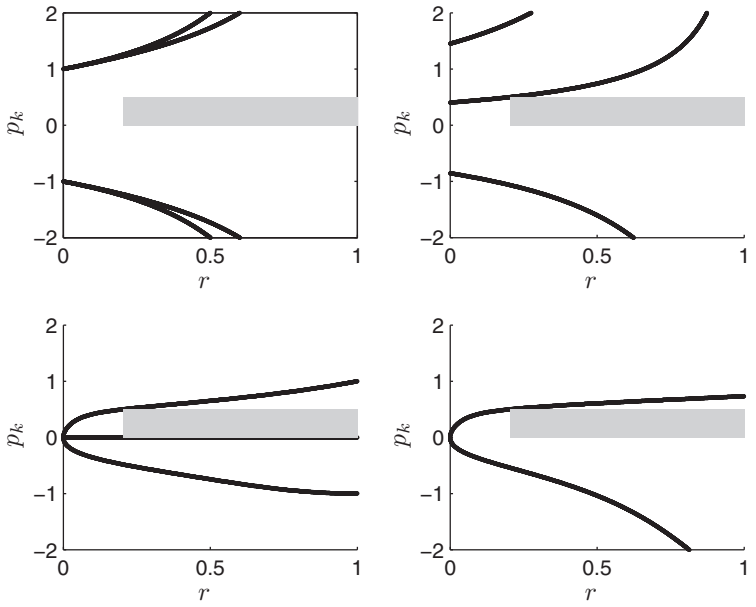

FIG. 7.1. *Solutions of* $\phi(p_i) = p_k^2(1-r)^2$ *for various values of* p_i, p_k, *and* r. *Top-left:* $p_i = p^{(1)}$. *Top-right:* $p_i = p^{(2)}$. *Bottom-left:* $p_i = p_k$. *Bottom-right:* $p_i = 1 - p_k$. *The region* R *has been lightly shaded.*

The cases $p_i = p^{(2)}$, $p_i = p_k$, and $p_i = 1 - p_k$ lead to the top-right, bottom-left, and bottom-right parts (respectively) of Figure 7.1, and the result follows. ∎

Acknowledgments. We are grateful to our colleagues Martin J. Gander, Felix Kwok, and Hui Zhang for useful discussions. We are also indebted to the anonymous referees for their helpful comments.

REFERENCES

[1] A. Alonso-Rodriguez and L. Gerardo-Giorda, *New non-overlapping domain decomposition methods for the time-harmonic Maxwell system*, SIAM J. Sci. Comput., 28 (2006), pp. 102–122.

[2] D. Bennequin, M. J. Gander, and L. Halpern, *A homographic best approximation problem with application to optimized Schwarz waveform relaxation*, Math. Comp., 78 (2009), pp. 185–223.

[3] P. Chevalier and F. Nataf, *Symmetrized method with optimized second-order conditions for the Helmholtz equation*, Contemp. Math., 218 (1998), pp. 400–407.

[4] Q. Deng, *An optimal parallel nonoverlapping domain decomposition iterative procedure*, SIAM J. Numer. Anal., 41 (2003), pp. 964–982.

[5] V. Dolean, M. J. Gander, and L. Gerardo-Giorda, *Optimized Schwarz methods for Maxwell's equations*, SIAM J. Sci. Comput., 31 (2009), pp. 2193–2213.

[6] V. Dolean, S. Lanteri, and F. Nataf, *Optimized interface conditions for domain decomposition methods in fluid dynamics*, Internat. J. Numer. Methods Fluids, 40 (2002), pp. 1539–1550.

[7] T. A. Driscoll, K.-C. Toh, and L. N. Trefethen, *From potential theory to matrix iterations in six steps*, SIAM Rev., (1998), pp. 547–578.

[8] S. W. Drury and S. Loisel, *The Performance of Optimized Schwarz and 2-Lagrange Multiplier Preconditioners for GMRES*, manuscript, 2013.

[9] O. Dubois, *Optimized Schwarz Methods for the Advection-Diffusion Equation and for Problems with Discontinuous Coefficients*, Ph.D. thesis, Department of Mathematics and Statistics, McGill University, Montreal, Canada, 2007.

[10] O. Dubois and S. H. Lui, *Convergence estimates for an optimized Schwarz method for PDEs with discontinuous coefficients*, Numer. Algorithms, 51 (2009), pp. 115–131.
[11] C. Farhat, A. Macedo, M. Lesoinne, F.-X. Roux, F. Magoulès, and A. de La Bourdonnaie, *Two-level domain decomposition methods with Lagrange multipliers for the fast iterative solution of acoustic scattering problems*, Computer Methods Appl. Mech. Engrg., 184 (2000), pp. 213–239.
[12] M. J. Gander, L. Halpern, and F. Nataf, *Optimized Schwarz methods*, in Proceedings of the 12th International Conference on Domain Decomposition, T. Chan, T. Kako, H. Kawarada, and O. Pironneau, eds., 2000, pp. 15–27.
[13] M. J. Gander, *Optimized Schwarz methods*, SIAM J. Numer. Anal., 44 (2006), pp. 699–731.
[14] M. J. Gander, *Schwarz methods in the course of time*, Electron. Trans. Numer. Anal., 31 (2008), pp. 228–255.
[15] M. J. Gander and L. Halpern, *Absorbing boundary conditions for the wave equation and parallel computing*, Math. Comp., 74 (2004), pp. 153–176.
[16] M. J. Gander and L. Halpern, *Optimized Schwarz waveform relaxation for advection reaction diffusion problems*, SIAM J. Numer. Anal., 45 (2007), pp. 666–697.
[17] M. J. Gander, L. Halpern, and C. Japhet, *Optimized Schwarz algorithms for coupling convection and convection-diffusion problems*, in Proceedings of the 13th International Conference on Domain Decomposition Methods, N. Debit, M. Garbey, R. Hoppe, J. Périaux, and Y. Kuznetsov, and D. Keyes, eds., 2001, pp. 253–260.
[18] M. J. Gander, L. Halpern, and F. Nataf, *Optimal convergence for overlapping and non-overlapping Schwarz waveform relaxation*, in Proceedings of the 11th International Conference on Domain Decomposition Methods, C.-H. Lai, P. E. Bjorstad, M. Cross, and O. Widlund, eds., 1999, pp. 27–36.
[19] M. J. Gander, L. Halpern, and F. Nataf, *Optimal Schwarz waveform relaxation for the one dimensional wave equation*, SIAM J. Numer. Anal., 41 (2003), pp. 1643–1681.
[20] M. J. Gander and F. Kwok, *Best Robin parameters for optimized Schwarz methods at cross points*, SIAM J. Sci. Comput., 34 (2012), pp. A1849–A1879.
[21] M. J. Gander, F. Magoules, and F. Nataf, *Optimized Schwarz methods without overlap for the Helmholtz equation*, SIAM J. Sci. Comput., 24 (2002), pp. 38–60.
[22] C. Japhet, *Conditions aux limites artificielles et décomposition de domaine: Méthode OO2 (optimisé d'ordre 2). Application à la Résolution de Problèmes en Mécanique des Fluides*, CMAP Ecole Polytechnique, Palaiseau, France, 373 (1997).
[23] C. Japhet, *Optimized Krylov-Ventcell method. Application to convection-diffusion problems*, in Proceedings of the Ninth International Conference on Domain Decomposition Methods, P. E. Bjørstad, M. S. Espedal, and D. E. Keyes, eds., 1998, pp. 382–389.
[24] C. Japhet, F. Nataf, and F. Rogier, *The optimized order 2 method. Application to convection-diffusion problems*, Future Generation Computer Systems, 17 (2001), pp. 17–30.
[25] J.-H. Kimn, *A convergence theory for an overlapping Schwarz algorithm using discontinuous iterates*, Numer. Math., 100 (2005), pp. 117–139.
[26] P.-L. Lions, *On the Schwarz alternating method* III: *A variant for non-overlapping subdomains*, in Third International Symposium on Domain Decomposition Methods for Partial Differential Equations, T. F. Chan, R. Glowinski, J. Périaux, and O. Widlund, eds., SIAM, Philadelphia, 1990, pp. 47–70.
[27] S. Loisel, J. Côté, M. J. Gander, L. Laayouni, and A. Qaddouri, *Optimized domain decomposition methods for the spherical Laplacian*, SIAM J. Numer. Anal., 48 (2010), pp. 524–551.
[28] S. Loisel and D. B. Szyld, *On the geometric convergence of optimized schwarz methods with applications to elliptic problems*, Numer. Math., 114 (2009), pp. 697–728.
[29] G. Lube, L. Mueller, and F.-C. Otto, *A non-overlapping domain decomposition method for the advection-diffusion problem*, Computing, 64 (2000), pp. 49–68.
[30] V. Martin, *An optimized Schwarz waveform relaxation method for unsteady convection diffusion equation*, Appl. Numer. Math., 52 (2005), pp. 401–428.
[31] V. Martin, *Schwarz waveform relaxation algorithms for the linear viscous equatorial shallow water equations*, SIAM J. Sci. Comput., 31 (2009), pp. 3595–3625.
[32] F. Nataf, *Absorbing boundary conditions in block Gauss-Seidel methods for convection problems*, Math. Models Methods Appl. Sci., 6 (1996), pp. 481–502.
[33] F. Nataf and F. Nier, *Convergence rate of some domain decomposition methods for overlapping and nonoverlapping subdomains*, Numer. Math., 75 (1997), pp. 357–377.
[34] A. Qaddouri, L. Laayouni, S. Loisel, J. Côté, and M. J. Gander, *Optimized Schwarz methods with an overset grid for the shallow-water equations: Preliminary results*, Appl. Numer. Math., 58 (2008), pp. 459–471.

[35] W. Ritz, *Über eine neue methode zur lösung gewisser variationsprobleme der mathematischen physik*, J. für die reine und angewandte Mathematik (Crelle), (1908), pp. 1–61.

[36] F.-X. Roux, *Optimization of interface operator based on algebraic approach*, in Domain Decomposition Methods in Science and Engineering, I. Herrera, D. E. Keyes, O. B. Widlund, and R. Yates, eds., Lecture Notes in Comput. Sci. and Engrg. 70, National Autonomous University of Mexico, 2002, pp. 297–304.

[37] A. Toselli and O. B. Widlund, *Domain Decomposition Methods – Algorithms and Theory*, Springer Series in Computational Mathematics 34, Springer Berlin Heidelberg, 2005.